

Crystal chemistry and phase composition of the MoVTeNbO catalysts for the ammoxidation of propane

M. Aouine,^a J. L. Dubois^b and J. M. M. Millet^{*a}

^a *Institute de Recherches sur la catalyse, CNRS, Conventionné à l'Université Claude-Bernard, Lyon I, 2 avenue Albert Einstein, 69626 Villeurbanne Cedex, France. E-mail: millet@catalyse.univ-lyon1.fr*

^b *Elf Atochem S.A. Centre de Recherches et développement de l'Est, B.P. 61005-57501 Saint-Avold Cedex, France*

Received (in Cambridge, UK) 1st May 2001, Accepted 16th May 2001

First published as an Advance Article on the web 8th June 2001

Unit cell parameters and space group symmetry have been determined for the two main phases of the MoVTeNbO catalysts; models of their structures are proposed based on electron micrographs, EDX data and comparison with other crystal structures.

New processes of production of acrylonitrile by ammoxidation of propane will be implemented on the industrial scale in the coming years.¹ Two catalytic systems, AlVSbWO and MoV-TeNbO have been shown to be effective and will most likely be used. The former has been extensively described in the literature whereas the latter has mostly been covered in the patent literature.¹⁻⁴

The presence in the MoVTeNbO catalyst of two major phases, denoted M1 and M2, has been shown to be key to obtain high yields.⁵ Very little is known about these phases whose presence has been verified almost exclusively employing X-ray diffraction. The role of these phases remains under debate mainly because none of these phases have been synthesised and studied independently.

We have synthesised a MoVTeNbO catalyst using a method described in the literature⁵ and characterised it by electron microscopy and X-ray diffraction. The catalyst was prepared from an aqueous slurry comprising Mo, V, Te and Nb in the ratios Mo:V:Te:Nb = 1:0.33:0.22:0.11, ratios most frequently reported in patent examples. The slurry was evaporated to dryness at 423 K and successively calcined at 573 K under air and 873 K under nitrogen for 2 h.

Powder X-ray diffraction patterns were obtained using a Siemens D5005 diffractometer and Cu-K α radiation. They were recorded with 0.02° (2 θ) steps over the angular range 3–88° with 16 s counting time per step. High-resolution electron microscopy was performed with a JEM 2010 ($C_s = 0.5$ mm). The accelerating voltage was 200 kV with a LaB₆ emission current, a point resolution of 0.195 nm and a useful limit of information of 0.14 nm. The instrument was equipped with an EDS LINK-ISIS (spatial resolution: 1 nm). An EDX study was conducted using a probe size of 25 nm to analyse isolated grains of the phases and avoid simultaneous analysis of grains of the two phases. Standard deviations were evaluated for atomic ratios from at least 20 analyses.

The X-ray diffraction pattern of the synthesised catalyst showed the sets of peaks reported in the literature for the two phases,¹ the more intense corresponding to the M2 phase. The electron diffraction spectra of the two phases have been indexed (Figs. 1 and 2). The M1 phase crystallises in the hexagonal system with possible space groups $P6mm$, $P\bar{6}m2$, $P622$ or $P6/mmm$ while phase M2 crystallises in the orthorhombic system. Extinction conditions observed for the latter are only compatible with the space group $P2_12_12$. The data obtained by electron microscopy made it possible to index the X-ray diffraction powder pattern of the phase mixture and to refine the cell parameters of the phases. The cell parameters of the M1 and M2 phases are, respectively, $a = 2.61(2)$, $c = 0.403(1)$ nm and $a = 2.1207(8)(3)$, $b = 2.6831(1)$ and $c = 0.8047(4)$ nm.

The structure of M1 is isomorphous to that of the phase Sb_{0.4}MoO_{3.1} reported by Parmentier *et al.*⁶ and corresponds to a hexagonal tungsten bronze structure.⁷ Although the structure is only partial; it can be schematized as shown in Fig. 3. Tellurium occupies the sites in the channels formed by the MO₆

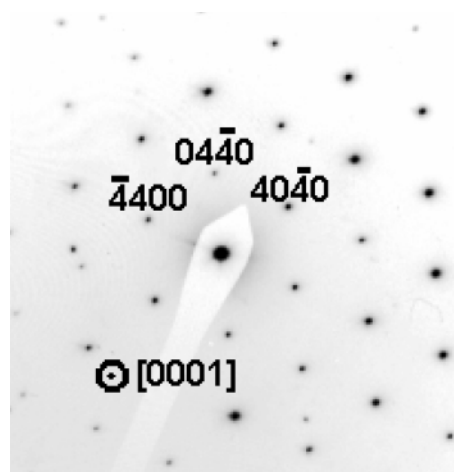


Fig. 1 Indexed electron diffraction pattern of the phase M1.

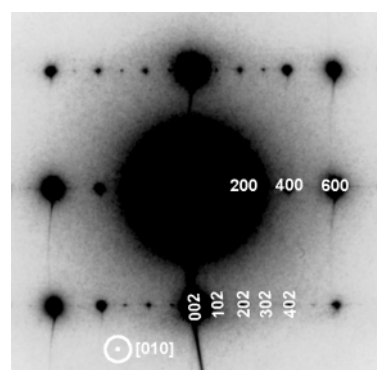


Fig. 2 Indexed electron diffraction patterns of the phase M2.

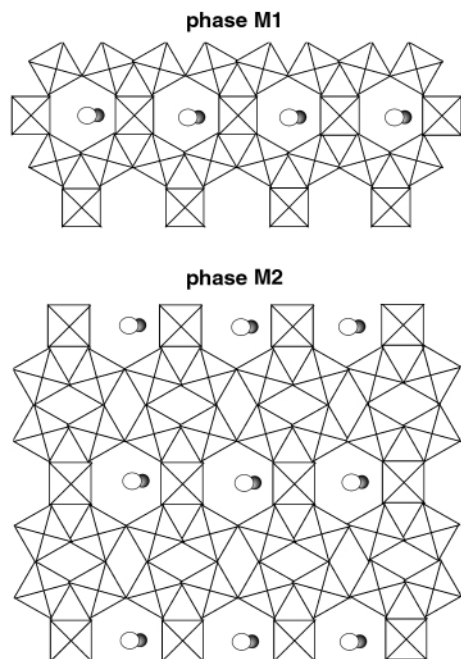


Fig. 3 Representation of the structures of the phases M1 and M2 along the *c* axis.

octahedra ($M = \text{Mo}, \text{V}, \text{Nb}$). In the case of the antimony bronze, it was proposed that Sb partially occupies the M sites which was not possible with Te, due to steric hindrance. Consequently the stoichiometry of the M1 phase should correspond to $\text{Te}_{0.33}\text{MO}_3$. Such stoichiometry is in accord with that calculated from EDX analyses (Table 1).

Table 1 EDX analyses of the two phases; standard deviations are given in parentheses

Phase	Te/Mo	V/Mo	Nb/Mo	Te/(Mo + V + Nb)	(Te + Nb)/(Mo + V)
M1	0.32(2)	0.30(2)	0.07(1)	0.23(4)	
M2	0.11(2)	0.23(2)	0.14(5)	0.08(4)	0.20(4)

The structure of M2 shows similarities with those of $\text{TeMo}_5\text{O}_{16}$ and $\text{Sb}_2\text{Mo}_{10}\text{O}_{31}$ (Table 2) and should present the atomic arrangement of $\text{TeMo}_5\text{O}_{16}$ (Fig. 3). A lattice image of the phase M2 taken with the incident beam parallel to the *b* axis shows an array of intense fringes having a separation of 1.04 nm (*i.e.* half of the *a* parameter) with in between streaks forming two less intense lines (Fig. 4). These fringes can respectively be attributed to the planes containing tellurium and molybdenum cations, as they appear in the structure model of $\text{TeMo}_5\text{O}_{16}$. The *a* parameters of the two phases (M2 and $\text{TeMo}_5\text{O}_{16}$) are quite similar, the *c* parameter of the former corresponds to twice that of the latter and the *b* parameter is *ca.* four times larger. These features could be related to a more

Table 2 Comparison of the unit cell parameters of the phase M2, $\text{Sb}_2\text{Mo}_{10}\text{O}_{31}$ and $\text{TeMo}_5\text{O}_{16}$

Phase	<i>a</i> /nm	<i>b</i> /nm	<i>c</i> /nm	Space group	Ref.
M2	2.1207(3)	2.6831(1)	0.8047(4)	$P2_12_12$	This study
$\text{Sb}_2\text{Mo}_{10}\text{O}_{31}$	2.023(1)	0.809(1)	0.717(1)	$Pma2$	8
$\text{TeMo}_5\text{O}_{16}$	2.0010(1)	0.72254(4)	0.40650(2)	$Pma/2$	9

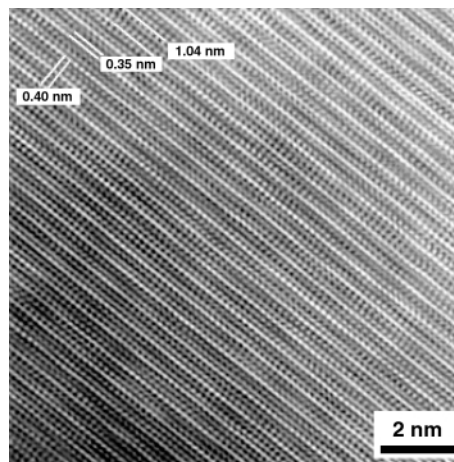


Fig. 4 High-resolution transmission electron imaging of the phase M2.

complex chemical composition of the M2 phase. Such a complex chemical composition should result from both the high degree of substitution of the molybdenum cations by the smaller vanadium cations and a possible ordering of the M cations on the sites. These features may also be due to the possible intergrowth of M2 and M1 structures as proposed earlier for $\text{TeMo}_5\text{O}_{16}$.¹⁰ The stoichiometry of the phase M2 should correspond to $\text{Te}_{0.2}\text{MO}_{3.2}$ (with $M = \text{Mo}, \text{V}$ and Nb). The stoichiometry calculated from EDX data with 0.08 Te per M cation does not agree well with this stoichiometry. It may be possible that niobium, which is in a larger amount in this phase, partially occupies the hexagonal window sites. The sub-stoichiometry in oxygen observed in the case of antimony is due to the absence of infinite chains $[\text{Te}-\text{O}]_\infty$ in the $[001]$ direction caused by a different orientation of the free electron pairs. This limits to three instead of four the number of oxygens neighboring the Sb cation. The presence of infinite chains could be an important parameter in the formation of this structure and explain the difficulties encountered when preparing the same catalysts with antimony in place of tellurium.

From the data generated from this study, the structures of the two phases can be described on the basis of two closely related stacking models. These models are built up from simple or double sheets of MO_6 ($M = \text{Mo}, \text{V}, \text{Nb}$) separated by rows of hexagonal windows occupied by tellurium cations (Fig. 3). These structures correspond to the same general formula $\text{Te}[\text{MO}_3]_{2n+1}$ with $n = 1$ for M1 and $n = 2$ for M2. This feature should explain why the two phases are systematically formed concomitantly.

Notes and references

- 1 M. Hatano and K. Kayou, *Eur. Pat.*, 318 295, 1988.
- 2 T. Ushikubo, K. Oshima, A. Kayo, T. Umezawa, K. Kiyono and I. Sawaki, *Eur. Pat.*, 529 853, 1992.
- 3 T. Ushikubo, K. Oshima, A. Kayou, T. Umezawa, K. Kiyono, I. Sawaki and H. Nakamura, *US Pat.*, US5472925; 1995.
- 4 H. Hinago and S. Komada, *Ger. Pat.*, DE19835247 A1, 1998.
- 5 T. Ushikubo, K. Oshima, A. Kayou and M. Hatano, *Stud. Surf. Sci. Catal.*, 1997, **112**, 473.
- 6 M. Parmentier, C. Gleitzer and R. J. D. Tilley, *J. Solid State Chem.*, 1980, **31**, 305.
- 7 A. Magneli, *Acta Chem. Scand.*, 1953, **7**, 315.
- 8 M. Parmentier, C. Gleitzer, A. Courtois and J. Protas, *Acta Crystallogr., Sect. B*, 1963, **35**, 1979.
- 9 P. Forestier and M. Geraud, *C.R. Acad. Sci. Paris Ser. II*, 1991, **312**, 1141.
- 10 S. Vallar and M. Geraud, *J. Solid State Chem.*, 1997, **129**, 303.